Photoemission and x-ray absorption of the electronic structure of multiferroic $R\mathrm{MnO_3}$ (R=Y,Er)

J.-S. Kang,[1,2,*] S. W. Han,[2] J.-G. Park,[2,3] S. C. Wi,[1] S. S. Lee,[1] G. Kim,[1] H. J. Song,[4] H. J. Shin,[4] W. Jo,[5] and B. I. Min[6]

[1]*Department of Physics, The Catholic University of Korea, Puchon 420-743, Korea*
[2]*CSCMR, Seoul National University, Seoul 151-742, Korea*
[3]*Department of Physics, Sungkyunkwan University, Suwon 440-746, Korea*
[4]*Pohang Accelerator Laboratory (PAL), POSTECH, Pohang 790-784, Korea*
[5]*Department of Physics, Ewha Womans University, Seoul 120-750, Korea*
[6]*Department of Physics, POSTECH, Pohang 790-784, Korea*

(Received 17 November 2004; revised manuscript received 18 January 2005; published 30 March 2005)

Electronic structures of multiferroic $R\mathrm{MnO_3}$ (R=Y,Er) have been investigated by employing photoemission spectroscopy (PES) and x-ray absorption spectroscopy (XAS). We have found that Mn ions in $R\mathrm{MnO_3}$ are in the trivalent high-spin state with the total spin of $S=2$. The occupied Mn ($d_{xz}-d_{yz}$) states lie deep below E_F, while the occupied Mn ($d_{xy}-d_{x^2-y^2}$) states overlap very much with the O 2p states. It is observed that the PES spectral intensity of Mn 3d states is negligible above the occupied O 2p bands, suggesting that $\mathrm{YMnO_3}$ is likely to be a charge-transfer insulator. The Mn $d_{3z^2-r^2}$ state is mostly unoccupied in the ferroelectric phase of $\mathrm{YMnO_3}$.

DOI: 10.1103/PhysRevB.71.092405 PACS number(s): 77.84.−s, 79.60.−i, 71.20.Eh

Hexagonal yttrium (Y) and rare-earth (R) manganites of the formula $R\mathrm{MnO_3}$ (R=Ho, Er, Tm, Yb, Lu, or Y) belong to an interesting class, known as multiferroic materials, in which the ferroelectric and magnetic ordering coexist at low temperatures.[1–4] Hexagonal $R\mathrm{MnO_3}$ compounds have antiferromagnetic ordering with the Neel temperature (T_N) of $T_N<70-130$ K,[1,5] and the ferroelectric ordering occurs at a high temperature ($T_E\sim 600-990$ K).[1,2] $R\mathrm{MnO_3}$ crystallizes in two structural phases; the hexagonal phase when the ionic radius of R is small, and the orthorhombic phase when the ionic radius of R is rather large. Note that the ferroelectric ordering occurs only in the hexagonal phase of $R\mathrm{MnO_3}$, while the magnetic ordering occurs in both hexagonal and orthorhombic phases. In the hexagonal structure, each Mn ion is surrounded by three in-plane and two apical oxygen ions, and so it is subject to a trigonal crystal field.[6] These $\mathrm{MnO_5}$ blocks are connected two dimensionally through their corners, and the triangular lattice of $\mathrm{Mn^{3+}}$ ions is formed. These hexagonal $R\mathrm{MnO_3}$ compounds experience characteristic distortions such as tilting of $\mathrm{MnO_5}$ blocks and the displacement of R^{3+} ions along the c axis, causing a ferroelectric polarization.[6,7]

There seems to be a strong coupling between the ferroelectric and magnetic ordering in hexagonal $R\mathrm{MnO_3}$ compounds. For example, a critical change of dielectric constants at T_N has been reported for $R\mathrm{MnO_3}$ polycrystalline samples,[8–10] suggesting a coupling between the ferroelectric and magnetic ordering. Further, the coupled antiferromagnetic and ferroelectric domains have been observed in $\mathrm{YMnO_3}$,[11] and the magnetic phase of $\mathrm{HoMnO_3}$ has been observed to be controlled by the electric field.[12] In the optical study of $\mathrm{LuMnO_3}$,[13] a strong coupling of antiferromagnetism to the optical absorption spectra has been observed.

Understanding the origin of the coexistence of magnetism and ferroelectricity in hexagonal $R\mathrm{MnO_3}$ is a fundamental physics question, but has not been well understood yet. The d^0-ness rule is generally accepted in ferroelectricity. That is, a ferroelectric displacement of the B cation in $AB\mathrm{O_3}$ is inhibited if the formal charge of the B ion does not correspond to a d^0 electron configuration due to the strong on-site Coulomb interaction between d electrons. In contrast, the occupancy of transition-metal d electrons is crucial in the magnetic ordering. Thus the simultaneous magnetic and ferroelectric ordering in $R\mathrm{MnO_3}$ seems to break the d^0-ness rule. It was suggested that the multiferroic property in $R\mathrm{MnO_3}$ is a result of the effective one-dimensional (1D) d^0-ness along the c axis.[14,15] According to the electronic structure calculations,[16,17] the $\mathrm{Mn^{3+}}$ ($3d^4$) ion in $\mathrm{YMnO_3}$ is not a Jahn-Teller ion since the highest occupied 3d level ($d_{xy}-d_{x^2-y^2}$) is nondegenerate because of the trigonal symmetry of the surrounding oxygen ions. The $d_{3z^2-r^2}$ state is mostly unoccupied so that this effective 1D d^0 orbital along the c axis allows ferroelectricity to occur via the usual ligand-field stabilization mechanism. This is a plausible idea, but has not been confirmed experimentally yet.

In order to understand the origin of the multiferroicity in hexagonal $R\mathrm{MnO_3}$, it is important to investigate the electronic structures of hexagonal $R\mathrm{MnO_3}$, including the valence states of Mn ions and the character of the lowest unoccupied 3d states of the Mn ion below and above the ferroelectric transition. In principle, these investigations are possible by employing the polarization-dependent soft x-ray absorption spectroscopy (XAS) and valence-band photoemission spectroscopy (PES) measurements. PES and XAS are powerful experimental methods for providing direct information on the electronic structures of solids. In practice, however, these spectroscopic measurements are not easy for these multiferroic materials. Normally these systems are good insulators having wide band gaps, and so they are not good for electron spectroscopy studies. For the polarization-dependent experiments, single crystals are prerequisite. Further, it is difficult to study the changes in the electronic structure across T_E

using these spectroscopy experiments because it is practically not compatible with the ultrahigh vacuum required for the experiments to achieve these high temperatures ($T_E \sim 600-990$ K).

In this paper, we report the valence-band PES, O 1*s* XAS, and Mn 2*p* XAS study of polycrystalline $R\mathrm{MnO_3}$ (R=Y,Er) samples at room temperature which belongs to the paramagnetic ferroelectric phase. To our knowledge, this is the first reliable PES and XAS study on multiferroic samples. Only the core-level PES data for the sputtered $\mathrm{YMnO_3}$ films have been reported so far.[18] This study provides the information on the electronic structures of $R\mathrm{MnO_3}$ (R=Y,Er) in their ferroelectric and paramagnetic phases even though we did not perform the polarization-dependent spectroscopy measurement across T_E or T_N.

Polycrystalline $R\mathrm{MnO_3}$ samples (R=Y,Er) were synthesized by using the standard solid-state reaction method. Cation oxides of $R_2\mathrm{O_3}$ (R=Y,Er) (99.999%) and $\mathrm{Mn_2O_3}$ (99.999%) were thoroughly mixed in order to achieve a homogeneous mixture. The mixed powders were heated to 900 °C for 12 h and later they were annealed at 1100 °C for 24 h and subsequently at 1200 °C for 24 h before final sintering at 1350 °C for 24 h with intermediate grindings. The purpose of intermediate grindings was to prevent the formation of impurity phases. The x-ray diffraction (XRD) measurements at room temperature showed that all the samples have a single hexagonal $R\mathrm{MnO_3}$ phase.

Valence-band PES, O 1*s* XAS, and Mn 2*p* XAS measurements were performed at the 8A1 undulator beamline of the Pohang Accelerator Laboratory (PAL). Samples were cleaned *in situ* by repeated scraping with a diamond file and the data were obtained at room temperature with the pressure better than 4×10^{-10} Torr. The Fermi level E_F (Ref. 19) and the overall instrumental resolution [full width at half maximum (FWHM)] of the system were determined from the valence-band spectrum of a scraped Pd metal in electrical contact with samples. The FWHM was about 100–400 meV between a photon energy $h\nu \sim 130$ eV and $h\nu \approx 600$ eV. All the spectra were normalized to the incident photon flux. The XAS spectra were obtained by employing the total electron yield method. The experimental energy resolution for the XAS data was set to ~100 meV at the O 1*s* and Mn 2*p* absorption thresholds ($h\nu \approx 500-600$ eV).

Figure 1 compares the Mn 2*p* XAS spectra of $R\mathrm{MnO_3}$ (R=Y,Er) to those of reference Mn compounds having formal Mn valences of 3+ ($\mathrm{Mn_2O_3}$, reproduced from Ref. 20), 4+ ($\mathrm{MnO_2}$ reproduced from Ref. 21), 2+ (MnO reproduced from Ref. 21), and that of Mn metal (reproduced from Ref. 22). The XAS data of $\mathrm{MnO_2}$, MnO, and Mn metal were shifted by −0.8, +1.0, and −1.3 eV, respectively, to allow for a better comparison of the data. It is well known that the peak positions and the line shape of the Mn 2*p* XAS spectrum depend on the local electronic structure of the Mn ion, so that the 2*p* XAS spectrum provides the information on the valence state of the Mn ion.[23,24] Figure 1 shows clearly that the Mn 2*p* XAS spectra of $R\mathrm{MnO_3}$ (R=Y,Er) are essentially identical to each other, and that they are very similar to that of $\mathrm{Mn_2O_3}$. For comparison, they are quite different from those of MnO (2+), $\mathrm{MnO_2}$ (4+), and Mn metal. This observation indicates that the valence states of Mn ions in $R\mathrm{MnO_3}$ are nearly trivalent ($\mathrm{Mn^{3+}}$), with the $3d^4$ configuration, but far from being divalent ($\mathrm{Mn^{2+}}, 3d^5$) or tetravalent ($\mathrm{Mn^{4+}}, 3d^3$). This finding is consistent with the finding of Mn *K*-edge XANES,[25] and with the general consensus of $\mathrm{Mn^{3+}}$ ions in the ionic bonding picture for hexagonal $R\mathrm{MnO_3}$.

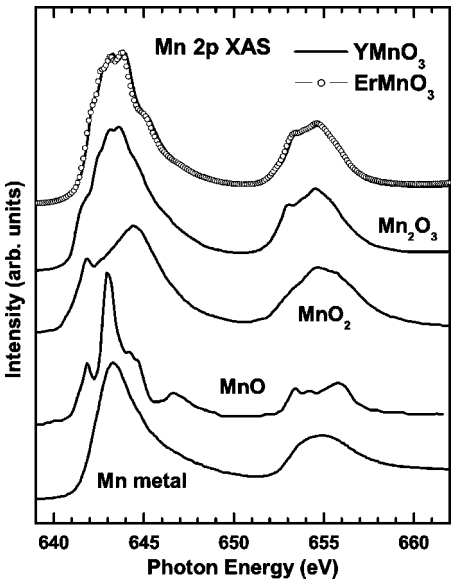

FIG. 1. Comparison of the Mn 2*p* XAS spectra of $\mathrm{YMnO_3}$ (solid lines) and $\mathrm{ErMnO_3}$ (symbols) to those of $\mathrm{Mn_2O_3}$ ($\mathrm{Mn^{3+}}$) (Ref. 20), $\mathrm{MnO_2}$ ($\mathrm{Mn^{3+}}$) (Ref. 21), MnO ($\mathrm{Mn^{2+}}$) (Ref. 21), and Mn metal (Ref. 22).

If Mn ions in $R\mathrm{MnO_3}$ have the $3d^4$ configurations, then the next question would be which states are occupied, which states are unoccupied, and where these states are located with respect to E_F. In order to answer these questions, we have investigated the photoemission spectral weight distribution of Mn 3*d* electrons, by employing resonant photoemission spectroscopy (RPES) near the Mn $2p \rightarrow 3d$ absorption threshold.

The top of Fig. 2 shows the valence-band RPES spectra of $\mathrm{YMnO_3}$ near the Mn $2p_{3/2}$ absorption edge. We have also done RPES measurements for $\mathrm{ErMnO_3}$, but the valence-band PES spectra have large contribution from Er 4*f* electron emissions, which overlap with both Mn 3*d* and O 2*p* emissions. So we do not present the PES data for $\mathrm{ErMnO_3}$ in this paper. The inset shows the Mn $2p_{3/2}$ XAS spectrum of $\mathrm{YMnO_3}$, and the arrows in the XAS spectrum represent $h\nu$'s where the valence-band spectra were obtained. The off-resonance valence-band PES spectrum (*A*) consists of both O 2*p* and Mn 3*d* electron emissions with comparable contributions, but has the negligible contribution from Y s/p electron emissions.[26] The top PES spectrum (labeled as XPS) was obtained with $h\nu$=1486.6 eV, which belongs to the XPS limit. This XPS spectrum is very similar to the off-resonance spectrum (*A*), because, at $h\nu$=1486.6 eV, the O 2*p* and Mn 3*d* electron emissions are also of comparable magnitudes.[26] The enhanced features near ~7 eV binding energy at the Mn $2p \rightarrow 3d$ absorption energy (*B*) represent the resonant Mn 3*d* electron emission. Therefore the difference between the on-resonance and off-resonance spectra can be considered to

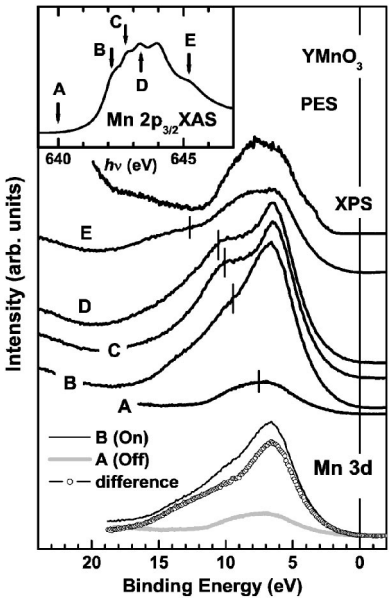

FIG. 2. Valence-band PES spectra of $YMnO_3$ near the Mn $2p_{3/2} \rightarrow 3d$ absorption edge. Inset: The Mn $2p_{3/2}$ XAS spectrum of $YMnO_3$. Arrows denote $h\nu$'s where the valence-band PES spectra were obtained. Bottom: Comparison of the on-resonance (solid line) and off-resonance valence-band PES spectra (gray line) in Mn $2p \rightarrow 3d$ RPES, and the difference between these two (open dots).

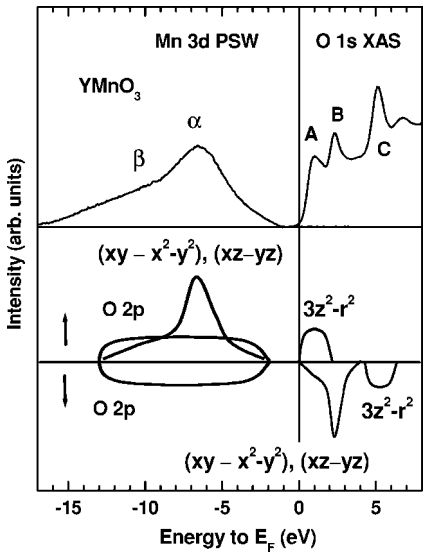

FIG. 3. Top: Combined Mn $3d$ PSW and O $1s$ XAS for $YMnO_3$. Bottom: The schematic diagram for the Mn $3d$ PDOS of $YMnO_3$. $\uparrow$ and $\downarrow$ represent the majority- and minority-spin states, respectively.

represent the *bulk* Mn $3d$ partial spectral weight (PSW) distribution.[27] The vertical bars, marked for those features that shift away from E_F with increasing $h\nu$, denote the Mn *LMM* Auger emission that appears at a fixed kinetic energy (KE) of KE $\sim$634 eV.[28] These Auger peaks also reveal the intensity enhancement near the Mn $2p$ absorption threshold. It is known that the transition-metal (T) Auger peaks show the resonant behavior near the T $2p \rightarrow 3d$ RPES.[29]

The bottom of Fig. 2 presents the extraction procedure of the Mn $3d$ PSW for $YMnO_3$. As a first approximation, it is taken as the difference between the Mn $2p \rightarrow 3d$ on-resonance spectrum (solid line) and off-resonance spectrum (gray line). In this extraction procedure, we have used the on-resonance spectrum at B, instead of C or D, to reduce the effect of the Mn Auger contribution. The extracted Mn $3d$ PSW exhibits a peak centered at $\sim$7 eV binding energy with an asymmetric and long tail to the high binding energy side (up to $\sim$15 eV). Part of this high binding tail is ascribed to the underlying Mn Auger peak. The extracted Mn $3d$ PSW for $YMnO_3$ shows that Mn $3d$ states are located well below E_F but that there is nearly no Mn $3d$ occupied states near E_F. Note that both the off-resonance spectrum (A) and the $h\nu$=1486.6 eV XPS spectrum represent a mixture of O $2p$ and Mn $3d$ emissions. Therefore the bottom part of Fig. 2 reveals that the occupied Mn $3d$ states lie in the middle of the O $2p$ states and that they overlap with the O $2p$ states very much, having the comparable widths to those of the O $2p$ states. This finding implies the strong hybridization between Mn $3d$ and O $2p$ states.

Figure 3 shows the combined Mn $3d$ PSW and the O $1s$ XAS spectrum of $YMnO_3$.[30] The O $1s$ XAS spectrum represents the transition from the O $1s$ core level to the unoccupied O $2p$ states which are hybridized with the other electronic states, so it provides a reasonable estimate of the unoccupied conduction bands. The peaks *A*, *B*, *C* in the O $1s$ XAS spectrum of $YMnO_3$ have also been observed in $ErMnO_3$ and they were very similar to each other, indicating that they have mainly the O $2p$-Mn $3d$ character. At the bottom of Fig. 3, we also provide a schematic diagram for the partial densities of states (PDOS) for $YMnO_3$. We have determined this schematic PDOS diagram through the comparison of the PES/XAS data and the LSDA+U band calculations (LSDA: local spin-density approximation, U: on-site Coulomb interaction) for $YMnO_3$.[16,17] Our PES/XAS data agree better with the LSDA+U calculations than with the LSDA calculations. This finding is plausible because the on-site Coulomb interaction between Mn d electrons is expected to be strong. But the employed U=8 eV in the existing LSDA+U calculations seems to be too large for $YMnO_3$, as discussed below.

The features observed in the PES/XAS are ascribed to the following states. α: the occupied Mn $3d$ states consisting of the narrow ($d_{xz}\uparrow - d_{yz}\uparrow$) states, which are superposed on top of the rather broad ($d_{xy}\uparrow - d_{x^2-y^2}\uparrow$) states, β (the high binding energy shoulder to α): the Mn Auger peak, $\alpha+\beta$ (the broad valence-band PES features underneath the Mn $3d$ states): the O $2p$ states. Note that the occupied O $2p$ states are hybridized with Mn ($d_{xy} - d_{x^2-y^2}$) states, consistent with the band-structure calculations.[16,17] In the XAS side, the marked peaks represent the following states. *A*: the unoccupied Mn $d_{3z^2-r^2}\uparrow$ states, *B*: the unoccupied Mn ($d_{xy}\downarrow - d_{x^2-y^2}\downarrow$) and ($d_{xz}\downarrow - d_{yz}\downarrow$) states, *C*: the unoccupied Mn $d_{3z^2-r^2}\downarrow$ states. Thus the state just above E_F corresponds to Mn $d_{3z^2-r^2}\uparrow$, and so the trivalent Mn^{3+} ions in $RMnO_3$ are in the high-spin state (S=2) with the configuration of $(d_{xz}\uparrow - d_{yz}\uparrow)^2(d_{xy}\uparrow - d_{x^2-y^2}\uparrow)^2$. Considering the uncertainty in the binding energy calibration of PES data,[19] the energy separation between the peak α in the valence-band PES and

the peak A in the O 1*s* XAS amounts to $7\sim8$ eV. Then this value gives a rough measure of $U+\Delta_{CF}$ (Ref. 31) (Δ_{CF}: the crystal-field splitting between $d_{3z^2-r^2}$ and $d_{xz}-d_{yz}$). Employing $\Delta_{CF}\approx2$ eV from the LSDA band structure calculation,[16] the estimated value of U would be of the order of 5–6 eV. Hence the present spectral data indicate that the Mn 3*d* Coulomb interaction U is not as large as that ($U=8$ eV) employed in Refs. 16 and 17. The energy separation (~2 eV) between the top of the valence band and the peak *A* in the O 1*s* XAS is expected to correspond to the lowest energy peak in the optical absorption spectrum for $YMnO_3$.[18,32] We ascribe this energy separation to the energy difference between the occupied O 2*p* states, which are strongly hybridized to the $(d_{xy}\uparrow-d_{x^2-y^2}\uparrow)$ states, and the unoccupied Mn $d_{3z^2-r^2}\uparrow$ states.

Note that the extracted Mn 3*d* PSW shows negligible spectral weight near E_F. Thus our schematic PDOS diagram shown in Fig. 3 implies that the topmost electronic states in the valence bands of $YMnO_3$ (those closest to E_F) are mostly O 2*p* states. According to this picture, the lowest-energy optical transition would be the O *p*-Mn *d* transition, suggesting that $YMnO_3$ is likely to be a charge-transfer insulator. Noteworthy is that our model for the electronic structure of $YMnO_3$ is different from that proposed from the optical absorption study of $LuMnO_3$,[13] where a sharp peak at 1.7 eV (even at room temperature) was ascribed to the on-site Mn *d*-*d* transition. In contrast, similar absorption peaks were observed in $RMnO_3$ ($R=$Sc, Y, Er), and they were interpreted as arising from charge transfer from O 2*p* to Mn 3*d* states.[32] The present PES/XAS data indicate that the latter interpretation is more consistent with the real electronic structures in $RMnO_3$.

In conclusion, the electronic structures of hexagonal multiferroic $RMnO_3$ ($R=$Y, Er) materials have been investigated by employing Mn $2p\rightarrow3d$ RPES, Mn 2*p* XAS, and O 1*s* XAS. The Mn 2*p* XAS spectra of $RMnO_3$ ($R=$Y, Er) show that Mn ions are in the formally trivalent Mn^{3+} states, implying the $(d_{xz}\uparrow-d_{yz}\uparrow)^2(d_{xy}\uparrow-d_{x^2-y^2}\uparrow)^2$ configurations with the total spin of $S=2$ per Mn ion. According to Mn $2p\rightarrow3d$ RPES for $YMnO_3$, the occupied Mn $(d_{xz}-d_{yz})$ states lie very deep below E_F, with a peak around ~7 eV binding energy. The occupied Mn $(d_{xy}-d_{x^2-y^2})$ states overlap with the O 2*p* states very much, but show negligible Mn 3*d* spectral weight above the O 2*p* states, suggesting that $YMnO_3$ is likely to be a charge-transfer insulator. The lowest unoccupied peak in the O 1*s* XAS is ascribed to the unoccupied Mn $d_{3z^2-r^2}$ state. This finding is compatible with the recent structural studies of $RMnO_3$,[6,7] which show tilting of MnO_5 blocks in their ferroelectric phases.

We thank S.-W. Cheong for helpful discussions. This work was supported by the KRF (Grant No. KRF-2002-070-C00038) and by the KOSEF through the CSCMR at SNU and the eSSC at POSTECH. The PAL is supported by the MOST and POSCO in Korea.

*Electronic address: kangjs@catholic.ac.kr

[1] E. F. Bertaut *et al.*, Acad. Sci., Paris, C. R. **256**, 1958 (1963).
[2] H. L. Yakei *et al.*, J. Appl. Crystallogr. **16**, 957 (1963).
[3] G. A. Smolenskii and I. E. Chupis, Sov. Phys. Usp. **25**, 475 (1982).
[4] H. Schmid, Ferroelectrics **162**, 317 (1994).
[5] W. C. Koehler *et al.*, Phys. Lett. **9**, 93 (1964).
[6] T. Katsufuji *et al.*, Phys. Rev. B **64**, 104419 (2001).
[7] B. B. van Aken *et al.*, Nat. Mater. **3**, 164 (2004).
[8] Z. J. Huang *et al.*, Phys. Rev. B **56**, 2623 (1997).
[9] N. Iwata and K. Kohn, J. Phys. Soc. Jpn. **67**, 3318 (1998).
[10] T. Kimura *et al.*, Nature (London) **426**, 55 (2003).
[11] M. Fiebig *et al.*, Nature (London) **419**, 818 (2002).
[12] T. Lottermoser *et al.*, Nature (London) **430**, 541 (2004).
[13] A. B. Souchkov *et al.*, Phys. Rev. Lett. **91**, 027203 (2003).
[14] N. A. Hill and A. Filippetti, J. Magn. Magn. Mater. **242-245**, 976 (2002).
[15] N. A. Spandin and W. E. Pickett, J. Solid State Chem. **176**, 615 (2003).
[16] J. E. Medvedeva *et al.*, J. Phys.: Condens. Matter **12**, 4947 (2000).
[17] M. Qian *et al.*, Phys. Rev. B **63**, 155101 (2001).
[18] W. C. Yi *et al.*, J. Phys. Soc. Jpn. **69**, 2706 (2000).
[19] Since $RMnO_3$ samples are insulating, there is some ambiguity in determining E_F. However, no time-dependent charging effects were observed in the valence-band PES spectra of $RMnO_3$. Therefore the absolute values of binding energies in these data have some uncertainties, but the relative energy separations are meaningful.
[20] P. Ghigna *et al.*, Phys. Rev. B **64**, 132413 (2001).
[21] C. Mitra *et al.*, Phys. Rev. B **67**, 092404 (2003).
[22] Y. Yonamoto *et al.*, Phys. Rev. B **63**, 214406 (2001).
[23] F. M. F. de Groot *et al.*, Phys. Rev. B **42**, 5459 (1990).
[24] G. van der Laan and I. W. Kirkman, J. Phys.: Condens. Matter **4**, 4189 (1992).
[25] C. T. Wu *et al.*, Physica B **329-333**, 709 (2003).
[26] J. J. Yeh and I. Lindau, At. Data Nucl. Data Tables **32**, 1 (1985), where calculated atomic photoionization cross sections are given.
[27] J.-S. Kang *et al.*, Phys. Rev. B **66**, 113105 (2002).
[28] *Handbook of Auger Electron Spectroscopy*, edited by C. L. Herdberg, 3rd ed. (Physical Electronics, Inc., Minnesota, 1995).
[29] J.-S. Kang *et al.*, Phys. Rev. B **68**, 012410 (2003).
[30] In this comparison, the inelastic background has been subtracted in the Mn 3*d* PSW, and the O 1*s* XAS spectrum has been shifted by −530 eV by referring to the optical gap size of $YMnO_3$.
[31] Here it is implicitly assumed that the occupied α and unoccupied A peaks correspond to the $d^n\rightarrow d^{n-1}$ and $d^n\rightarrow d^{n+1}$ transitions, respectively.
[32] A. M. Kalashnikova and R. V. Pisarev, JETP Lett. **78**, 143 (2003).